Journal of Biomolecular Structure and Dynamics

ISSN: 0739-1102 (Print) 1538-0254 (Online) Journal homepage: http://www.tandfonline.com/loi/tbsd20

Molecular modeling and spectroscopic studies of semustine binding with DNA and its comparison with lomustine–DNA adduct formation

Shweta Agarwal, Deepti Chadha & Ranjana Mehrotra

To cite this article: Shweta Agarwal, Deepti Chadha & Ranjana Mehrotra (2015) Molecular modeling and spectroscopic studies of semustine binding with DNA and its comparison with lomustine–DNA adduct formation, Journal of Biomolecular Structure and Dynamics, 33:8, 1653-1668, DOI: 10.1080/07391102.2014.968874

To link to this article: http://dx.doi.org/10.1080/07391102.2014.968874

Journal of Biomolecular Structure and Dynamics, 2015
Vol. 33, No. 8, 1653–1668, http://dx.doi.org/10.1080/07391102.2014.968874

Molecular modeling and spectroscopic studies of semustine binding with DNA and its comparison with lomustine–DNA adduct formation

Shweta Agarwal, Deepti Chadha and Ranjana Mehrotra*

Quantum Phenomenon and Applications, CSIR-National Physical Laboratory, Dr. K. S. Krishnan Marg, New Delhi 110012, India

Communicated by Ramaswamy H. Sarma

(*Received 12 July 2014; accepted 21 September 2014*)

Chloroethyl nitrosoureas constitute an important family of cancer chemotherapeutic agents, used in the treatment of various types of cancer. They exert antitumor activity by inducing DNA interstrand cross-links. Semustine, a chloroethyl nitrosourea, is a 4-methyl derivative of lomustine. There exist some interesting reports dealing with DNA-binding properties of chloroethyl nitrosoureas; however, underlying mechanism of cytotoxicity caused by semustine has not been precisely and completely delineated. The present work focuses on understanding semustine–DNA interaction to comprehend its anti-proliferative action at molecular level using various spectroscopic techniques. Attenuated total reflection–Fourier transform infrared (ATR-FTIR) spectroscopy is used to determine the binding site of semustine on DNA. Conformational transition in DNA after semustine complexation is investigated using circular dichroism (CD) spectroscopy. Stability of semustine–DNA complexes is determined using absorption spectroscopy. Results of the present study demonstrate that semustine performs major-groove-directed DNA alkylation at guanine residues in an *incubation-time–drug-concentration-dependent* manner. CD spectral outcomes suggest partial transition of DNA from native B-conformation to C-form. Calculated binding constants (K_a) for semustine and lomustine interactions with DNA are $1.53 \times 10^3\ M^{-1}$ and $8.12 \times 10^3\ M^{-1}$, respectively. Moreover, molecular modeling simulation is performed to predict preferential binding orientation of semustine with DNA that corroborates well with spectral outcomes. Results based on comparative study of DNA-binding properties of semustine and lomustine, presented here, may establish a correlation between molecular structure and cytotoxicity of chloroethyl nitrosoureas that may be instrumental in the designing and synthesis of new nitrosourea therapeutics possessing better efficacy and fewer side effects.

Keywords: semustine; lomustine; molecular modeling; FTIR spectroscopy; CD spectroscopy; Drug–DNA interaction

Introduction

DNA, the genetic material of cell, is associated with several vital biological processes such as replication, transcription, and recombination. These auxiliary processes and DNA itself can be targeted with small molecules or ligands that may hold antitumor activity (Kennard, 1993; Haq & Ladbury, 2000). Therefore, understanding physical and chemical interaction properties of DNA and ligands has become essential (Chaires, 1998). Interaction studies have shown to be important to elucidate a correlation between molecular structure of the drugs and their anticancer activity (González-Ruiz et al., 2011; Mehrotra et al., 2013). Results of such investigations may help in the designing and synthesis of new drugs with fewer side effects and more specificity (Nandy & Basak, 2010). One of the major classes of cancer chemotherapeutics is alkylating agents, which are used in the treatment of various types of cancer, viz multiple myeloma, sarcoma, and lymphoma (Puyo, Montaudon, & Pourquier, 2013). Semustine or [1-(2-chloroethyl)-3-(4-methylcyclohexyl)-1-nitrosourea] (Figure 1(a)) is a member of chloroethyl nitrosourea (CENU) family. It is a 4-methyl derivative of lomustine or CCNU ([1-(2-chloroethyl)-3-cyclohexyl-1-nitrosourea] (Figure 1(b)), also designated as methyl-CCNU (Boice et al., 1983). It is used as an antineoplastic alkylating agent to treat various types of malignancy including Lewis lung carcinoma, leukemia, and metastatic brain tumor. Semustine is also used to treat Hodgkin lymphoma, malignant melanoma, and lung carcinoma (McCormick & Stanley McElhinney, 1990; Schabel, 1976). Semustine has lipophilic nature that enables its distribution quickly across the tissues (Miyagami, Tsubokawa, Tazoe, & Kagawa, 1990). This lipophilic property allows it to cross the blood–brain barrier for the chemotherapy of gliomas (Boice et al., 1983; Miyagami et al., 1990). It has been shown that semustine interacts with cellular DNA of highly dividing cells (McCormick & Stanley McElhinney, 1990). CENUs are considered to exert their anticancer activity by stimulating the formation of DNA interstrand cross-links (ICLs) (Bai, Zhao, & Zhong, 2010). Zhao and his colleagues have demonstrated the comparative investigation among different CENUs

*Corresponding author. Email: ranjana@mail.nplindia.ernet.in

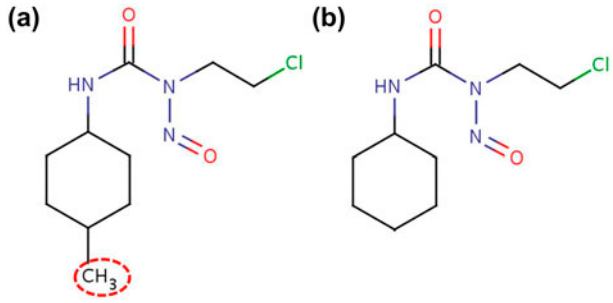

Figure 1. Chemical structure of (a) semustine and (b) lomustine. Red dotted circle contrasts the presence of methyl group in semustine.

(nimustine, carmustine, lomustine, and fotemustine), regarding their ICLs activity with respect to their stability in aqueous solution. They have also established a correlation between ICLs activity of CENUs with their reported anticancer efficiency (Zhao, Li, Xu, & Zhong, 2014; Zhao, Ren, Bai, Zhang, & Zhong, 2011). Hayes et al. studied a correlation between the exposure time of CENUs to DNA and level of ICLs formed, using agarose gel electrophoresis. Their results demonstrated that increasing the exposure time led to an increase in the quantity of ICLs formed (Hayes, Bartley, Parsons, Eaglesham, & Prakash, 1997). Baoqing and his group quantified dG-dC cross-links in oligonucleotide duplexes induced by CENUs using HPLC/ESI-MS/MS method (Bai, Zhao, & Zhong, 2011). There exist several reports, which present the result of various investigations conducted on the binding mechanism of CENUs with DNA (Gombar, Tong, & Ludlum, 1980; Naghipur, Ikonomou, Kebarle, & Lown, 1990; Schallreuter, Gleason, & Wood, 1990; Zhao, Zhong, & Zhen, 2007). Nevertheless, detailed structural aspects, on the direct interaction of semustine with DNA, are still obscure. Therefore, it is of great importance to elucidate the peculiarities of semustine–DNA complexation.

It has been reported that the binding site and binding affinity of a drug with its target are mainly governed by various non-covalent interactions (Snyder, Holt, Maguire, & Trent, 2013). In view of this, we have performed molecular modeling of semustine with DNA to predict its preferential orientation and binding properties (Huang & Zou, 2010; Morris et al., 1998b, 2009). Moreover, in the last few years, spectroscopic techniques such as infrared (IR) and circular dichroism (CD) have shown the potential to characterize the nature of various biomolecules and their complexes, particularly for their molecular structural information (Agarwal, Jangir, & Mehrotra, 2013; Jangir, Kundu, & Mehrotra, 2013; Tyagi, Charak, & Mehrotra, 2012). Precisely, attenuated total reflection–Fourier transform infrared (ATR-FTIR) spectroscopy has shown remarkable potential in deciphering the binding characteristics of various drug–DNA complexes (Jangir, Charak, Mehrotra, & Kundu, 2011; Agarwal, Jangir, Singh, & Mehrotra, 2014). Most importantly, ATR-FTIR spectroscopy enables the environment modulation of the biomolecule so that structural and conformational transition can be studied as a function of temperature and pH to mimic the physiological conditions (Braun et al., 2003). In addition, CD spectroscopy reveals the details on the degree of conformational alteration in DNA after its complexation with drug (Kypr, Kejnovská, Renčiuk, & Vorlíčková, 2009). Binding mode and stability of drug–DNA complexes can be assessed using UV–visible spectroscopic technique (Braun et al., 2003). Hence, with the present work, the competency of ATR-FTIR, CD, and UV–visible spectroscopy is used to evaluate various binding parameters of semustine–DNA complex.

We report a comparative study on the DNA-binding properties of semustine (methyl-CCNU) and lomustine (CCNU) with respect to their interaction mode, preferential binding site and stability of their adduct with DNA. Semustine and lomustine differ in their molecular structure by only one methyl group, nevertheless show different cellular activity related to their initial binding site on target molecule. As both of these CENUs are anti-chemotherapeutic agents and used in the treatment of various tumors, detailed comparative study on their preferential interaction site and subsequent intracellular action requires attention. Such relative assessment gives a glimpse of *structure–function relationship* of the drug. Further, these results may provide an input for rational drug designing of new chloroethyl nitrosourea derivatives with anti-cancer potential.

Materials and methods

Materials

Semustine (M.W. –247.7) and highly polymerized type I calf thymus DNA (sodium content 6%) are procured from Sigma Aldrich chemicals, USA. To estimate DNA purity, the absorbance ratio of DNA at 260 nm (A_{260}) and 280 nm (A_{280}) is calculated. The ratio of (A_{260})/(A_{280}) is found to be 1.83, which suggests sufficient purity of DNA (Glasel, 1995). Deionized water (resistance 18.2 MΩ) from the Scholar-UV Nex UP 1000 system is used for the preparation of buffer and semustine drug solutions. Other chemicals and reagents utilized in this investigation are of analytical grade.

Stock solutions preparation

DNA stock solution is prepared in tris-HCl buffer (10 mM, pH 7.4) and placed at 8 °C for about 24 h. This solution is stirred at regular time intervals to ensure the homogeneity of DNA solution. Using molar extinction coefficient of 6600 cm^{-1} M^{-1}, final concentration of

DNA stock solution is measured spectrophotometrically (Vijayalakshmi, Kanthimathi, Subramanian, & Nair, 2000) and is found to be 42 mM (due to phosphate group molarity).

In silico study

The 3D structure of DNA dodecamer d(CGCGAATTCGCG)$_2$–benzimidazole complex is taken from RCSB Protein Data Bank in PDB format (PDB ID: 453d) (Neidle et al., 1999). Benzimidazole is unhooked from the DNA–benzimidazole complex (453d) using UCSF Chimera (Huang, Couch, Pettersen, & Ferrin, 1996). The 3D files of semustine (ID: 3831006) and lomustine (ID: 3874951) are obtained from Zinc database (Irwin, Sterling, Mysinger, Bolstad, & Coleman, 2012) in mol2 format, which are then converted to PDB format using off-line version of Open Babel 3.2.9 (O'Boyle et al., 2011). AutoDock (version 4.2) is used for molecular docking simulations (Morris et al., 2009). The Lamarckian genetic algorithm (LGA) is adopted to perform the molecular docking studies (Morris et al., 1998). B-DNA (453d) is used as a rigid input receptor molecule for docking, whereas semustine and lomustine are used as flexible ligands and number of active torsions are set to 4 (Goodsell, Morris, & Olson, 1996). AutoDockTools version 1.5.6 (ADT) is used to prepare the receptor and the ligand coordinate files in PDBQT format, as required by AutoGrid and AutoDock for further simulations (Sanner, 1999). Grid maps are computed using AutoGrid considering grid box of dimension $62 \times 62 \times 20$ with .375 Å spacing. The grid center coordinates for semustine and lomustine are set to 15.111, 20.786, and 13.837 and 15.111, 20.786, and 19.05, respectively. The docking parameters used for modeling are listed in Table 1. A ranked cluster analysis employing ADT is performed on docking results for conformational analysis. All the 100 docked conformations are analyzed, and structurally similar conformations are grouped into clusters, ranked in the order of increasing energy using RMSD tolerance of 2.0 Å (Sanner, 1999). The lowest-energy docked conformer is considered to be the best result and is used to further analyze the molecular interactions of semustine and lomustine with DNA (Morris et al., 1998; Huey & Morris, 2008).

Table 1. Molecular docking parameters.

Docking parameters	Value
Number of individuals in population	150
Maximum number of energy evaluations	2,500,000
Maximum number of generations	27,000
Number of top individuals to survive to next generation	1
Rate of cross over	.8
Rate of gene mutation	.02
Number of hybrid GA-LS or LGA runs	100

FTIR spectroscopy

For the FTIR spectroscopic investigation of free calf thymus DNA and semustine–DNA complexes, Varian-660-IR spectrophotometer is used. This instrument is equipped with deuterated triglycine sulfate (DTGS) detector and KBr beam splitter. To remove water vapors from sample chamber, dry nitrogen gas is purged continuously. Miracle® (PIKE) ZnSe-micro horizontal attenuated total internal reflection (HATR) assembly is used for the sampling in ATR mode. During experiments, ambient humidity of 46% RH is maintained. For the spectral measurements of semustine–DNA complexes, drug solutions of three different concentrations (.525, 1.05, and 4.2 mM) are prepared. Thereafter, these drug solutions are added in a dropwise manner to DNA solution (42 mM) to achieve 1/80, 1/40, and 1/10 M ratios (r) of semustine–DNA complexes. Continuous vortexing for 15 min followed by incubation at room temperature for different periods (2, 4, 6, 8, and 24 h) is performed to ensure the complete complexation of semustine with DNA. Two-hundred and fifty-six interferograms are collected in the spectral range of 2400–700 cm^{-1} with a resolution of 2 cm^{-1}. Before each spectral measurement, background atmospheric spectrum is collected. Multiple baseline corrections and normalization for DNA band at 968 cm^{-1} are employed. To perform water subtraction, a spectrum of tris buffer (10 mM) is recorded and then subtracted from the spectra of free DNA and semustine–DNA complexes. An acceptable water subtraction is regarded to be achieved, when the intensity of water combination band at ~2200 cm^{-1} becomes zero in the spectra of free DNA and drug–DNA complexes (Alex & Dupuis, 1989).

CD spectroscopy

CD spectra are recorded on Applied Photophysics (Chirascan) spectrophotometer. Spectral measurements are taken using quartz cuvette having a pathlength of 1 mm in the far UV range (200–320 nm). All the spectra are collected at room temperature subsequent to varying degree of incubation time (2, 4, 6, 8, 12, and 24 h) of semustine with calf thymus DNA. Six scans are recorded with a scanning speed of 1 nm/s and then averaged for each sample. Spectrum of buffer is subtracted from the spectra of free DNA and semustine–DNA complexes to accomplish buffer subtraction. For CD spectral measurements, semustine solution of varying concentration (in the range of .0625–.5 mM) are prepared and added into DNA solution of constant concentration (5 mM) and thus, drug/DNA molar ratios (r) become 1/80, 1/40, and 1/10.

UV–visible spectroscopy

The absorption spectra of free DNA and its complexes with CENUs (semustine and lomustine) are recorded on Perkin-Elmer Lambda-35 spectrophotometer. For UV–visible studies, .2 mM DNA solution is used with varying concentration of CENUs ranging from 2×10^{-1} to 2×10^{-2} mM. Quartz cuvette with a pathlength of 1 cm is used for the measurements. Binding constants (K_a) for the formation of CENUs–DNA complexes are calculated assuming that only one type of interaction occurs between DNA (D) and drug (S) in aqueous solution resulting in the formation of one type of complex (DS) (Connors, 1991). It is also presumed that DNA and ligand follow Lambert–Beer's law for the absorbance of light. The absorbance of DNA solution (A_0) at its total concentration (D_t) with a path length (l) of 1 cm is:

$$A_0 = \varepsilon_D l D_t \tag{1}$$

where ε_D is the molar absorptivity of free DNA.

The absorbance of solution (A_S) comprising of total concentration of DNA (D_t) along with total concentration of drug (S_t) is:

$$A_S \rightarrow \varepsilon_D l[D] + \varepsilon_S l[S] + \varepsilon_{DS} l[DS] \tag{2}$$

where

$[D]$ is the concentration of uncomplexed DNA.
$[S]$ is the concentration of uncomplexed drug.
$[DS]$ is the concentration of drug–DNA complex.
ε_s is the molar absorptivity of drug.
ε_{DS} is the molar absorptivity of drug–DNA complex.

After combining with the mass balance of DNA and drug, the absorbance equation can be written as:

$$A_S \rightarrow \varepsilon_D l\, D_t + \varepsilon_S l\, S_t + \Delta\, \varepsilon_{DS}\, l\, [DS] \tag{3}$$

$$\Delta\varepsilon_{DS} \rightarrow \varepsilon_{DS} - \varepsilon_D - \varepsilon_S$$

The absorbance of solution (A) measured against the total concentration of drug as reference is

$$A \rightarrow \varepsilon_D\, l\, D_t + \Delta\varepsilon_{DS}\, l\, [DS] \tag{4}$$

The stability constant (K_{DS}) for the formation of complex (DS) can be given as

$$K_{DS} \rightarrow [DS]/[D][S] \tag{5}$$

Combining Equations (4) and (5)

$$\Delta A \rightarrow K_{DS}\, \Delta\varepsilon_{DS} l[D][S] \tag{6}$$

$$\Delta A = A - A_0$$

From the mass balance equation $D_t = [D] + [DS]$, we get $[D] = D_t/(1 + K_{DS}[S])$, that gives following equation:

$$\frac{\Delta A}{l} \rightarrow \frac{D_t K_{DS}\, \Delta\varepsilon_{DS}[S]}{1 + K_{DS}[S]} \tag{7}$$

There is a hyperbolic relation between the free drug molecule concentration and its interaction with DNA. Linear transformation of Equation (6) is done by taking the reciprocal of both side of Equation (7) that can be presented as:

$$\frac{l}{\Delta A} \rightarrow \frac{1}{D_t K_{DS}\, \Delta\varepsilon_{DS}[S]} + \frac{1}{D_t \Delta\varepsilon_{DS}} \tag{8}$$

The double-reciprocal plot of $1/\Delta A$ vs. $1/[S]$ is linear, and the binding constant (K) can be calculated by estimating the ratio of the intercept to the slope.

Results and discussion

Molecular docking analysis of semustine–DNA complex

Figure 2(a) and (b) illustrate the docked model of semustine with DNA. In the semustine–DNA docking simulation of 100 runs, the majority of the binding conformers (66 poses) are obtained in the DNA major groove, in contrast to 34 conformers in the DNA minor groove. In addition, the most populated cluster, with 33 docked conformations; also belong to the major groove. These, all together, can predict the major-groove-directed binding of semustine (Figure 2(a)). To further analyze the molecular level properties of semustine–DNA complexation (using ADT), the lowest-energy docked conformer in major groove is selected, shown in Figure 2(b). Docking study reveals that semustine interacts with DNA through thymine, guanine, and cytosine nitrogenous bases. Moreover, the docked model (Figure 2(b)) depicts the formation of two hydrogen bonds, first is between the 2nd oxygen atom of semustine (acceptor residue) and H41 of 21st cytosine (donor residue) having 1.803 Å distance whereas 1st oxygen atom of ligand (acceptor) is forming second hydrogen bond with cytosine (H41) at 3rd position (donor residue) with 2.045 Å distance. Besides this, van der Waals interactions, in the semustine–DNA docked model, are analyzed using ADT and presented as spheres in the form of thin wireframes on those pairs of atoms that are closer than the sum of their van der Waals radii (Figure 2(b)). This establishes the contribution of hydrogen bonds (ΔG_{hbond}) and van der Waals forces (ΔG_{vdw}) in the overall binding free energy of semustine with DNA (Table 2). The predicted binding free energy for semustine–DNA complexation, that is, –4.4 kcal/mol is in good agreement to that of the experimental value (–4.35 kcal/mol) estimated from UV–visible spectral outcome (Morris et al., 1998). Furthermore, in AutoDock, the structure-based scoring

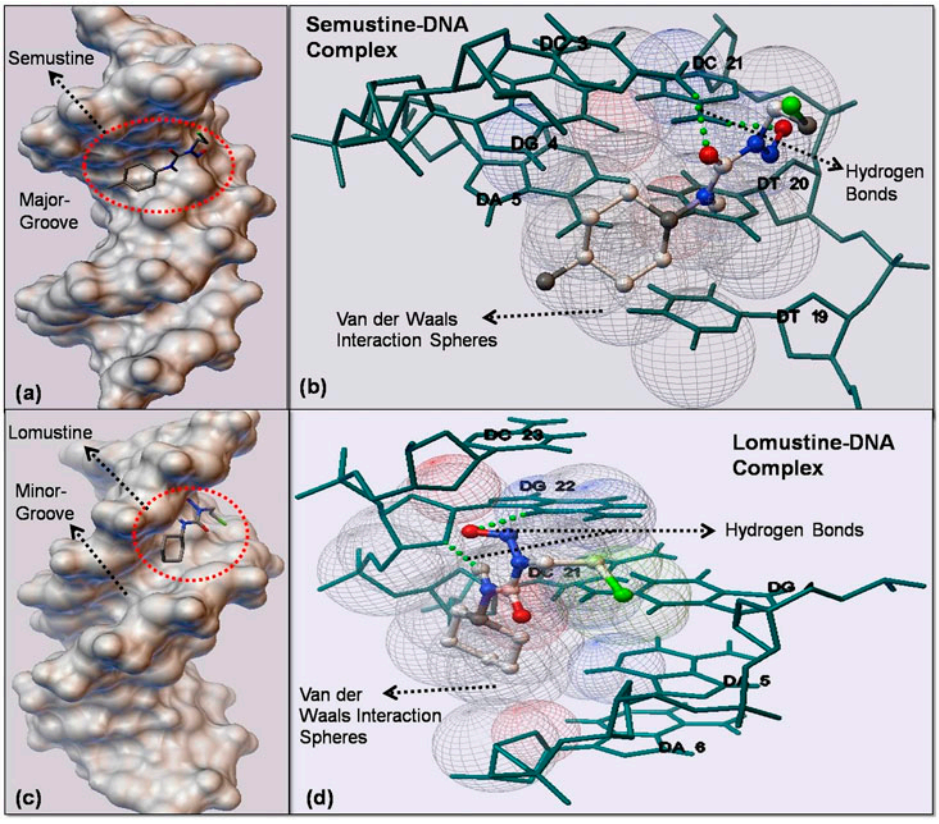

Figure 2. (a) The docked model of semustine with DNA illustrating the major-groove-directed binding of ligand. (b) The lowest-energy docked conformer of semustine–DNA complex (in major groove) revealing the interaction of semustine with DNA through thymine, guanine, and cytosine nitrogenous bases. Moreover, the docked model depicts the formation of two hydrogen bonds between the oxygen atom at 2nd position of semustine (acceptor residue) and H41 of cytosine at 21st position (donor residue) having distance 1.803 Å, while oxygen atom at 1st position of ligand (acceptor residue) is interacting with cytosine (H41) at 3rd position (donor residue) with distance 2.045 Å. Besides this, van der Waals interactions are analyzed using ADT and presented here as spheres in the form of thin wireframes on those pairs of atoms that are closer than the sum of their van der Waals radii. (c) Docked conformer of lomustine–DNA complex exhibiting DNA minor-groove-oriented binding of ligand. (d) The best docked structure of lomustine and DNA based on minimum binding energy. It shows the direct interaction of lomustine with DNA nitrogenous bases, guanine, and cytosine. This conformer exhibited two hydrogen bonds; hydrogen atom at 12th position of lomustine (donor residue) forms hydrogen bond with O4′ of deoxyribose sugar moiety (acceptor residue) linked to guanine at 22nd position having distance 2.09 Å, whereas oxygen atom at 2nd position of ligand (acceptor residue) is interacting with guanine (H3) at 22nd position (donor residue) with distance 2.037 Å.

Table 2. Predicted binding free energy values (kcal/mol) for lowest-energy docked conformer of CENUs with dodecamer d $(CGCGAATTCGCG)_2$.

Drug	Predicted Binding Free Energy ΔG_{bind}[a]	Final Intermolecular Energy ΔG_{inter}[b]	vdW + hBond + desolvation Energy* $\Delta G_{vdw + hbond + desolv}$	Electrostatic Energy ΔG_{elec}	Total Internal Energy ΔG_{total}	Torsional Free Energy ΔG_{tor}	Unbound System's Energy ΔG_{unb}	Experimentally Calculated Energy ΔG_{obs}
Semustine	−4.40	−5.59	−5.57	−.02	+.05	+1.19	+.05	−4.35
Lomustine	−6.36	−7.55	−7.57	+.02	+.16	+1.19	+.16	−5.33

[a] $\Delta G_{bind} = \Delta G_{inter}$[b] $+ \Delta G_{total} + \Delta G_{tor} - \Delta G_{unb}$.
[b] $\Delta G_{inter} = \Delta G_{vdw + hbond + desolv} + \Delta G_{elec}$.
* $\Delta G_{vdw + hbond + desolv}$ is the sum of van der Waals energy (ΔG_{vdw}), hydrogen bond energy (ΔG_{hbond}), and desolvation energy (ΔG_{desolv}).

method employs empirical free energy functions for the prediction of interaction between ligands and their macromolecular targets. However, the free energy of binding (ΔG_{bind}) is modeled in terms of dispersion and repulsion (ΔG_{vdw}), hydrogen bond (ΔG_{hbond}), desolvation (ΔG_{desolv}), electrostatic (ΔG_{elec}), torsional free energy

(ΔG_{tor}), final total internal energy (ΔG_{total}), and unbound system's energy (ΔG_{unb}) (Morris et al., 1998). This may be written as:

$$\Delta G_{bind} = \Delta G_{vdw} + \Delta G_{hbond} + \Delta G_{desolv} + \Delta G_{elec} + \Delta G_{tor} + \Delta G_{total} - \Delta G_{unb}$$

Further, it has been reported that favorable binding between receptor and ligand is majorly driven by the electrostatic, hydrogen bond, hydrophobic, and van der Waals interactions (Strange, 1996). Referring to Table 2, the degree of electrostatic energy (ΔG_{elec}), that is, –.02 kcal/mol is very less, which proposes negligible contribution of electrostatic interactions in case of semustine–DNA complexation. Besides this, desolvation free energy (ΔG_{desolv}), which models desolvation upon ligand binding, is used as a measure of hydrophobic forces (Aksel, Majumdar, & Barrick, 2011; Morris et al., 1998; Rueda, Banerjee, Aziz, & Raza, 2010). Furthermore, it is difficult to differentiate the individual contribution of hydrophobic and van der Waals forces in ligand–receptor binding, since van der Waals forces may also add interactions between nonpolar (aromatic and aliphatic) species (Strange, 1996). Here, AutoDock simulation results provide the sum of van der Waals, hydrogen bond, and desolvation energies ($\Delta G_{vdw} + \Delta G_{hbond} + \Delta G_{desolv}$) as a single value, which is predicted as –5.57 kcal/mol (Table 2). The docking analysis, presented here, illustrates van der Waals interactions, hydrogen bonds, and hydrophobic forces rather than electrostatic forces that are governing semustine–DNA complexation.

FTIR spectroscopic analysis

DNA nitrogenous base binding

Spectroscopic investigation of semustine–DNA complexes is performed to validate docking results. FTIR spectrum of free semustine is collected (Figure 4) and subtracted from drug–DNA complex spectrum. This is done to ensure that observed spectral variations in DNA are due to semustine binding. Besides this, IR spectral measurements for all the molar ratios of semustine–DNA complexes are recorded with respect to different incubation time ranging from 2 to 24 h to get more insights of semustine anti-cancer action mechanism. Figures 5 and 6 show infrared spectral characteristics observed in the spectrum of free calf thymus DNA and semustine–DNA complexes. Stretching vibrations due to nitrogenous bases (C=O, C=N), deoxyribose pentose sugar, and phosphate groups (PO_2 asymmetric and symmetric) of DNA occur in the spectral range of 1800–700 cm^{-1}. In-plane stretching vibrations of guanine (*G*) due to C6=O6 and C6=N1 bonds in DNA major groove lead to emergence of infrared bands at 1713 and 1574 cm^{-1}, respectively. The band at 1654 cm^{-1} is assigned to thymine (T) stretching vibrations, which correspond to C4=O4 bonds. The bands at 1492 and 1609 cm^{-1} are ascribed to the stretching vibrations of cytosine (C=C) and adenine (C=N), respectively. In addition, in-plane stretching vibrations owed to C4=NH2 bonds of cytosine in DNA major groove induces the appearance of infrared band at 1297 cm^{-1}. The infrared band at 1526 cm^{-1} is attributed to in-plane stretching vibrations of guanine and cytosine base pair (Banyay, Sarkar, & Gräslund, 2003).

After the addition of semustine into DNA, IR spectral features associated with nitrogenous bases exhibit a variation pattern in an *incubation-time–drug-concentration*-dependent manner. The infrared band at 1654 cm^{-1}, which is accredited to thymine (C4=O4 bonds in DNA major groove), demonstrates major spectral upshift of 7 cm^{-1} at highest semustine concentration (R-1/10) after 2 h of drug–DNA incubation (Figure 5(a)). This spectral shift is also accompanied with the deviation in intensity as evident by the positive band at 1652 cm^{-1} in the difference spectra of semustine–DNA complexes [(DNA solution + semustine solution) – DNA solution] (Figure 5(b)). Furthermore, it has been noticed that as the incubation time increases, spectral variations for thymine in terms of IR band shift and intensity become reduced (manifested by the IR band at 1654 cm^{-1} in Figure 6(a) and (c)). Besides this, a minor downshift of 1 cm^{-1} is observed for guanine band at 1713 cm^{-1} in the spectra of semustine–DNA complexes following 2 h of incubation (Figure 5(a)). With the increase in incubation time, spectral variations (band shift and intensity) for guanine enhance as apparent by IR band at 1708 cm^{-1} depicting downshift of 5 cm^{-1} (Figure 6(a)) and by the sharp negative band at 1719 cm^{-1} signifying decrease in intensity of guanine stretching vibrations (Figure 6(b)). Moreover, ensuing to 8 h of semustine–DNA incubation, IR spectral alterations for guanine becomes stable as obvious by the 1708 cm^{-1} IR band (Figure 6(c)) and 1722 cm^{-1} negative band (Figure 6(d)) in drug–DNA spectra following 24 h of incubation. In addition, cytosine exerts spectral variations similar to guanine. Till 4 h of semustine–DNA incubation, IR band 1492 cm^{-1}, ascribed to cytosine, demonstrates negligible shift and intensity variation as manifested by the presence of band at 1492 cm^{-1} (Figure 5(a)) and 1491 cm^{-1} (Figure 5(c)). Consequent to 8 h of incubation (Figure 6(a)), highest spectral shift (4 cm^{-1} downshift) and intensity change (positive band at 1484 cm^{-1}) is noticed for cytosine, which further becomes stable following 24 h of semustine–DNA incubation (Figure 6(c)). Along with the spectral variations (shifts and intensity change), percent effect of semustine binding with respect to different molar ratios and incubation periods on IR bands representative of reactive sites of DNA nitrogenous bases is depicted in Figure 7.

Spectral changes observed in terms of shifts and intensity deviations of base vibrations of DNA helix suggest the direct binding of semustine to heterocyclic base pair of DNA with major emphasis on thymine (band at 1654 cm^{-1}), guanine (band at 1713 cm^{-1}), and cytosine (band at 1492 cm^{-1}) (Ahmad, Arakawa, & Tajmir-Riahi, 2003). Adenine band at 1609 cm^{-1} neither underwent a shift in its position nor experienced any change in its infrared absorption intensity, signifying that semustine–DNA interaction is independent of adenine participation. Based on the infrared spectral analysis in conjunction with docking study, it can be inferred that semustine does not directly bind to guanine bases rather it initially interacts with thymine (C4=O4) residues in order to make proper contact with DNA duplex and subsequently performs its antitumor action. This preliminary binding may be carried out by hydrophobic forces exerted by the methyl group of semustine (Banerjee et al., 2014). In addition, C4=O4 group of thymine is located within DNA major groove; hence, it can be suggested that semustine performs major-groove-oriented action (Agarwal, Jangir, Mehrotra, Lohani, & Rajeswari, 2014). Preliminary binding of semustine with DNA may be followed by nucleophilic attack of 2-chloroethyl moiety of the drug on O6 position of guanine, resulting in the formation of O6-chloroethyl guanine adducts. Subsequently, O6-chloroethyl guanine may undergo intramolecular rearrangement to stimulate the formation of N1-O6 ethano-guanine adducts (Gombar et al., 1980; Naghipur et al., 1990; Tong, Kirk, & Ludlum, 1983). This adduct formation can be traced by the spectral variation at 1574 cm^{-1} infrared band, ascribed to C6=N1 stretching vibrations of guanine residues in DNA major groove (Figure 6(a) and (c)) (Banyay et al., 2003). Subsequently, N1-O6 ethano-guanine adduct may react with N3 of cytosine in the complementary strand of DNA to produce dG-dC interstrand cross-links (1-(3-cytosinyl)-2-(1-guanosinyl)-ethane) (Gombar et al., 1980; Naghipur et al., 1990; Tong et al., 1983). This is evident from the spectral alterations of IR bands at 1526 and 1297 cm^{-1}, which are accredited to in-plane stretching vibrations of guanine and cytosine base pair and C4-NH2 group of cytosine in DNA major groove, respectively (Figure 6(a) and (c)) (Banyay et al., 2003). In addition, it has been observed that spectral variations for the IR bands of cytosine and guanine are increased progressively with the incubation time, tending toward a steady state at about 8 h. Such spectral alteration can be the aspect of *critical time*, which is required by the ligand or drug molecule to exert its action mechanism entirely. Therefore, it can be proposed that anti-cancer action of semustine takes place in two phases: induction phase and execution phase. Induction phase is characterized by the preliminary binding of drug with thymine (C4=O4 group) in DNA major groove leading toward the buffering stage for the formation of O6-chloroethyl guanine adducts, as apparent by the minor shift and intensity variation for IR bands at 1713 cm^{-1} (guanine C6=O6), 1492 cm^{-1} (cytosine C=C), and 1297 cm^{-1} (cytosine C4-NH2) (Figure 5). Induction phase is followed by the execution phase, which is designated by an augmentation in the dG-dC interstrand cross-links formation (Figure 6). This is further affected by the semustine concentration, as the highest drug concentration (R-1/10) not only accelerates the rise of dG-dC interstrand cross-links, rather also favors the shortening of induction period. The dG-dC DNA interstrand cross-links formation, induced by semustine, finally attained a maximum steady state after 8 h (Tang, Zhao, & Zhong, 2008). Additionally, it can be presumed that induction phase is more significant as it forms the grounds for the subsequent anti-cancer action of semustine (i.e., DNA cross-linking). Moreover, cross-links generated by semustine induce the partial denaturation of DNA duplex, which can arrest the normal functions of DNA such as replication, transcription, and recombination in the cells and may cause cell death. This is in accordance with the previous reported investigations that "cross-links induced by DNA alkylating agent can locally destabilize the double helix followed by the opening of duplex" (Lenglet & David-Cordonnier, 2010; McCann, Lo, & Webster, 1971). This investigation concludes that semustine induces major-groove-directed DNA alkylation and produces dG-dC interstrand cross-links of DNA (however, it goes through two phases). In addition, the degree of cross-linking augments with the incubation time in a drug-concentration-reliant manner, which at the end achieves a stable form (Tang et al., 2008).

DNA phosphate–sugar backbone binding

In the FTIR spectrum of free DNA (Figures 5 and 6), the bands at 1083 and 1219 cm^{-1} are due to symmetric and asymmetric stretching vibrations of phosphate group, respectively (Banyay et al., 2003). The IR band at 1219 cm^{-1} consistently shows no appreciable shift except 1–2 cm^{-1} upon semustine complexation with DNA at all through the range of incubation time from 2 to 24 h. Besides this, the band at 1083 cm^{-1} (accredited to phosphate symmetric stretching vibrations) manifests similar spectral variations as exhibited by 1219 cm^{-1} band (upper panels of Figures 5 and 6). In the FTIR difference spectra, slight infrared hyperchroism is observed at 1206 and 1080 cm^{-1} (Figure 5(d)) that signifies minor alteration in intensity of phosphate stretching vibrations in DNA after its interaction with semustine. Similarly, in the IR spectrum of free DNA, infrared bands at 968 and 1052 cm^{-1} refer to C–C and C=O deoxyribose sugar stretching vibrations, respectively (Banyay et al., 2003). Utmost 1–2 cm^{-1} spectral shift is noticed for the bands at

1052 cm^{-1} and at 968 cm^{-1} after drug–DNA complex formation (Figure 6(a)). Moreover, both of these bands (968 and 1052 cm^{-1}) show an enhancement in intensity as manifested by positive spectral features at 962 and 1046 cm^{-1} in the difference spectra (Figure 5(d)). Infrared bands at 1372 and 780 cm^{-1} are assigned to C2′/C3′ endo–anti- and main N-type C3′ endo–anti-sugar conformations, respectively. In addition, the band at 725 cm^{-1} is ascribed to out-of-plane stretching vibrations of C3′ endo/anti-sugar conformation (Banyay et al., 2003). These bands show minor shift of 1 cm^{-1} when semustine–DNA interaction takes place. This minor shift is accompanied with slight variation in intensity in sugar stretching vibrations as indicated by positive bands at 1385, 780, and 724 cm^{-1} in the difference spectra of semustine–DNA complexes (Figure 5(d)). These spectral outcomes indicate toward minor external binding of semustine with DNA duplex through sugar–phosphate backbone (Agarwal, Jangir, Singh et al., 2014; Jangir et al., 2011).

DNA conformation

Infrared band at 837 cm^{-1}, attributed to C_2 endo–anti-/S-type-sugar pucker–phosphodiester stretching vibrations, is considered as a primary marker band for B-form of DNA (Figure 6(a)). In addition, the infrared bands at 893 cm^{-1} (due to pentose ring stretching vibrations) and 1219 cm^{-1} (due to PO2 antisymmetric stretching vibrations) also signify DNA conformation in B-form. Besides this, the IR bands at 1422 and 936 cm^{-1} are ascribed to C2′ endo deoxyribose sugar conformation in B-form helices. Moreover, one of the main DNA conformational component, that is, β-C/N-glycosidic linkage is denoted by the emergence of band at 1456 cm^{-1} (Banyay et al., 2003). Furthermore, the shoulder pattern, generated by the IR bands at 1083 and 1052 cm^{-1}, is the key indicator for proper DNA hydration value (Jangir et al., 2013; Loprete & Hartman, 1993; Pohle et al., 2000). After the formation of semustine–DNA complex, minor shift of 2–3 cm^{-1} is observed at these conformational infrared bands (1219, 893, 837, 1422, and 1457 cm^{-1}) (Figures 5 and 6). This minor shift is accompanied with the skewed manifestation of shoulder as the deeper minimum is observed at 1070 cm^{-1}, which signifies lower level of DNA hydration ensuing its resemblance to the spectrum of C-conformation (Figure 6(a)) (Loprete & Hartman, 1993; Pohle et al., 2000). However, these spectral alterations are observed in conjunction with the presence of B-conformation marker bands. Therefore, it can be concluded that semustine complexation with DNA duplex induces slight dehydration leading to the development of some C-form features, which subsequently forms a transitional state in double helix (B–C-conformation) (Agarwal et al., 2014).

CD spectroscopic analysis

Spectral changes in CD for calf thymus DNA in the absence and presence of increasing amount of semustine are recorded as a function of time to get detailed insights in the alkylation mechanism and subsequently induced conformational transition in DNA molecule (Figure 8). Helix with right-handedness and β-C/N-glycosidic linkages with asymmetrical arrangement of B-form of DNA give rise to a characteristic CD spectrum, which consists of positive as well as negative elliptical components: positive bands (at 277 nm and 223 nm) and negative bands (at 248 nm and 214 nm). Positive band at 277 nm emerges due to stacking interaction between nitrogenous bases of DNA, while second positive band at 223 nm signifies hydrogen bonds occurring between bases of complementary strands. Negative band at 248 nm indicates right-handedness of B-DNA double helix, whereas other negative band at 214 nm arises due to the β-C/N-glycosidic bond occurring between nitrogenous base and deoxyribose sugar (Johnson, 1994; Miyahara, Nakatsuji, & Sugiyama, 2012). Variation in these typical band positions and in ellipticity indicates corresponding conformational transitions in DNA double helix owing to its interaction with a ligand or drug (Kypr et al., 2009).

CD spectra, collected after 2 h of incubation of semustine and DNA, exhibit a spectacular alterations at all the molar ratios. The band accredited to base stacking interaction (at 277 nm) manifests enhancement in molar ellipticity in conjunction with 4-nm hypsochromic shift (273 nm) in a *drug-concentration-dependent* manner as maximum ellipticity is observed at higher semustine concentrations (R-1/10 and 1/40). Besides this, the band at 248 nm (assigned to DNA helicity) is intensified along with a slight blue shift of 1 nm upon the interaction of semustine with DNA. Nevertheless, the maximum magnitude of negative ellipticitical component (247 nm) is observed at the highest semustine–DNA molar ratio (R-1/10). The other dichroic components at 223 nm (assigned to hydrogen bonding between bases of complementary strands) and 214 nm (signifying β-C/N-glycosidic bond) demonstrate minor increase in molar ellipticity at all the molar ratios along with no spectral shift. These dichroic spectral changes may designate initial alterations in DNA duplex due to its interaction with semustine and reflect the formation of a reversible drug–DNA complex, in which semustine attempts to make stable contact with nucleic acid (Agarwal et al., 2014). Further, it can be suggested that this preliminary complexation is driven by non-covalent interactions of semustine with thymine (C4=O4) in DNA major groove as also evident by IR spectral shift and intensity variation at 1654 cm^{-1} band during the beginning hours of incubation (Figure 5(a)). Following the 4 h of incubation, CD spectra of semustine–DNA complexes reveal

dichroic aspects similar to that of 2 h except that maximum positive ellipticity (at 277 nm, green line) is manifested by the lowest drug concentration (R-1/80). Moreover, the band at 248 nm, referred to B-DNA duplex helicity, shows more pronounced spectral shift (blue shift of 2 nm) and ellipticity change (45% intensification) at all the molar ratios. Therefore, it is concluded that dichroic pattern exhibited by semustine–DNA complexes is *drug-concentration* and *incubation-time* dependent, since the trend pursued by lower molar ratio (R-1/80) at 4 h of incubation has been previously followed by the higher molar ratios (R-1/10 and 1/40) at 2 h of incubation. CD spectral attributes, observed at 6 h of DNA incubation with semustine, evolve into a variable-cum-stable form and demonstrate single isodichroic (isosbestic) point at 258 nm. These outcomes provide the spectral evidence for the development of a reactive intermediate in semustine–DNA reaction and system in equilibrium consisting of bound and free drug molecules (Brahms, Brahms, & Van Holde, 1976; Li, 2012). At 8 h of incubation of semustine–DNA complexes, CD spectra exhibited maximum changes in dichroic components ellipticity and position. After the interaction of semustine with DNA (at 8 h), the band at 277 nm (ascribed to base stacking interaction) exhibits an augmentation in ellipticity (93%) at all the molar ratios; nevertheless, this ellipticity variation is accompanied with no spectral shift. Besides this, the band at 248 nm (right-handed helicity of B-DNA) exhibits intensification (70%) along with 2-nm hypsochromic shift. Based on these spectral variations, it can be proposed that semustine complexation with DNA induces mild distortion in base stacking and slight deviation in local base-pair geometry of double helix. Moreover, the molar ellipticity at 277 nm possesses a linear correlation with DNA winding angle and propeller twist, as its augmentation (molar ellipticity at 277 nm) induces the reduction in DNA winding angle (opening of DNA duplex locally) and enhancement in DNA propeller twist (Chan, Kilkuskie, & Hanlon, 1979). Subsequently, alteration in these native properties of B-DNA (winding angle and propeller twist) causes small change in number of base pairs per turn in DNA duplex (Patil & Rhodes, 2000; Portugal & Subirana, 1985). Therefore, altogether, these spectral alterations make a prospect for the transition of native DNA conformation from B-form (10.4 base pair/helical turn) to C-form (9.2 base pair/helical turn) (Bokma, Curtis, & Blok, 1987; Portugal & Subirana, 1985; Zhang, Huang, Tang, Wang, & Dong, 2002). However, this transition appears to be limited up to few base pairs of DNA as for the complete transformation from B- to C-form, ellipticity at 248 nm must be in the exact ratio of two-third (66%) to that of B-DNA band, while here, we observed 70% intensification (Bokma et al., 1987; Brahms, Pilet, Lan, & Hill, 1973; Portugal & Subirana, 1985). Thereby, there is a possibility for the formation of a B–C-intermediate conformation of DNA duplex that possesses features of both B- and C-form (as apparent from FTIR spectral results). Besides this, hypsochromic shift and intensification at 248 nm band is also associated with the reduction in DNA hydration that runs along the inner edges of major groove around phosphate group. Further, it has been reported that guanine is hydrogen bonded to a water molecule from C6=O6 group in DNA major groove with single hydration on the free ring nitrogen atom N7-major groove. In addition, thymine is hydrogen bonded to a water molecule from C4=O4 group in major groove (Berman & Schneider, 1999; Degtyareva, Wallace, Bryant, Loo, & Petty, 2007; Woods, Lan, McLaughlin, & Williams, 2003). Moreover, increase in propeller twist or decrease in DNA winding angle (as evident from spectral alteration at 277 nm band) is accounted for DNA groove widening that facilitates the appropriate positioning of ligands within groove pocket (Agarwal et al., 2014). Therefore, it can be suggested that semustine interacts with DNA via hydrophobic forces and primarily binds with thymine residues (C4=O4 group) within DNA major groove ensuing the distortion of well-organized water network. Subsequently, it results in slight DNA dehydration, which induces structural transition (establishment of B–C-intermediate form) and reduction in free energy essential for DNA twisting leading to DNA denaturation (Berman & Schneider, 1999). This is supported by the fact that "alkylating agents may destabilize the DNA duplex by means of base flipping, DNA bending, and/or double-helical strand opening" (Lenglet & David-Cordonnier, 2010). Besides this, CD spectra of semustine–DNA complexes illustrate isoelliptic behavior at 231 and 258 nm (isosbestic points shown by red circles in Figure 8). This can be ascribed to semustine induced two-state transition in DNA molecule (Mayer & Drago, 1976; Kankia, Barany, & Musier-Forsyth, 2005), as semustine exerts its anti-cancer mechanism of action in two phase (formation of O6-chloroethyl guanine adducts pursued by the development of dG-dC DNA cross-links). Further, this is in corroboration with the FTIR spectral outcomes that signify an initial interaction of semustine with thymine followed by the formation of dG-dC DNA cross-links. In addition, other CD bands at 223 nm (accredited to hydrogen bonds occurring between purine and pyrimidine of complementary strands) and 214 nm (ascribed to β-C/N-glycosidic bond) manifest slight enhancements in their molar ellipticity accompanied with no spectral shift after the interaction of semustine with DNA. This change in molar ellipticity at 223 nm is ascribed to slight disturbance in hydrogen bonding, which may be a consequent of dG-dC DNA cross-links formation. Furthermore, the change in elliptical behavior of dichoric component at 214 nm can be outcome of the deviation in DNA

propeller twist that may influence β-C/N-glycosidic bond orientation (Agarwal et al., 2013, 2014). In addition, it has been observed that CD spectral variations accomplish a steady state after 8 h of incubation.

UV–visible spectroscopic analysis

Binding mode

The absorption spectra of free calf thymus DNA and its complexes with varying concentrations of CENUs (semustine and lomustine) are shown in Figure 9. The absorption spectra of DNA manifested quite similar behavior on addition of semustine and lomustine. When CENUs interact with DNA, they cause hyperchromic effect with increasing concentration of drugs in solution. This hyperchromic effect can be assigned to the binding of semustine and lomustine to DNA followed by base alkylation (Tyagi, Jangir, Singh, & Mehrotra, 2010; Tyagi et al., 2012). Alkylated base residues may generate interstrand cross-links that result in localized distortion and denaturation in double helix (as evident from FTIR and CD spectral outcome). This localized deformation may induce more exposure of bases to UV radiation, which leads to an enhancement in the absorption of UV radiation (Tyagi et al., 2010, 2012).

Binding strength of CENUs–DNA complexes

The binding constant (K_a) is calculated for the quantitative measurement of binding of semustine and lomustine with DNA. It is calculated by observing the changes in optical density at 260 nm for free DNA (represented by A_0) and its complexes with CENUs (represented by A). It includes the preparation of a series of drug–DNA complex solutions in which the concentration of DNA is held constant, while the drug concentration [C] is varied from 2×10^{-1} to 2×10^{-2} mM. The double-reciprocal plot of 1/ (A–A_0) versus 1/ [C] is linear and the binding constant (K_a) can be estimated from the ratio of intercept to slope (intersect of Figure 9). The binding constants

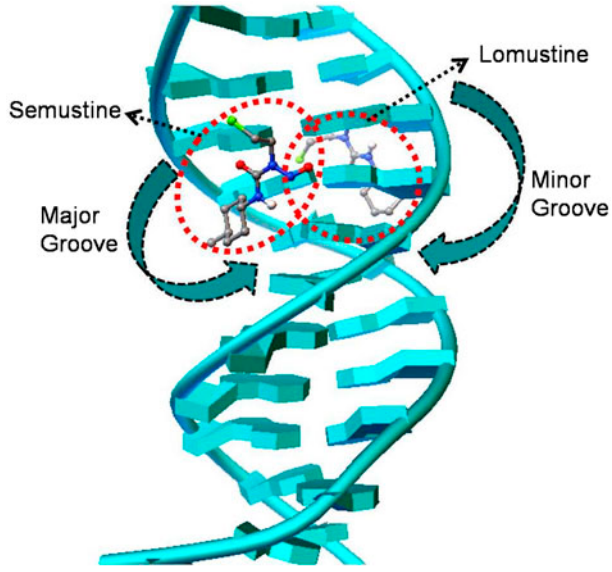

Figure 3. The docked model of semustine–DNA and lomustine–DNA, having duo CENUs in the superimposed position.

(K_a) for the interaction of semustine and lomustine with DNA are 1.53×10^3 M^{-1} and 8.12×10^3 M^{-1}, respectively, which indicate moderate type of CENU's binding with DNA duplex (Tyagi et al., 2012). Furthermore, it has been observed that the stabilities of both drug's complexes with DNA exhibit a little difference (though in the same range 10^3), which can be accredited to the slight molecular structural change between the two CENUs. Besides this, free energy for CENUs binding to DNA can be calculated using the following relation:

$$\Delta G_{\text{obs}} = -RT\ln K_a$$

where ΔG_{obs} is the observed binding free energy, R is the gas constant (1.987 cal K^{-1} mol^{-1}), T is the absolute temperature (298.15 K), and K_a is the binding constant. In the case of semustine, the value of K_a is 1.53×10^3 M^{-1}, thereby

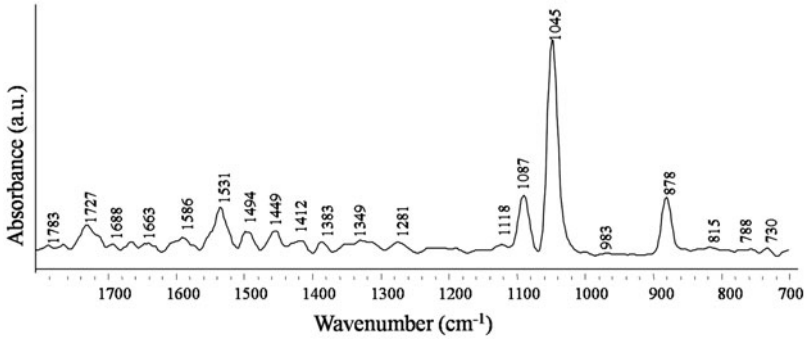

Figure 4. FTIR spectrum of semustine in the region of 1800 to 700 cm^{-1}.

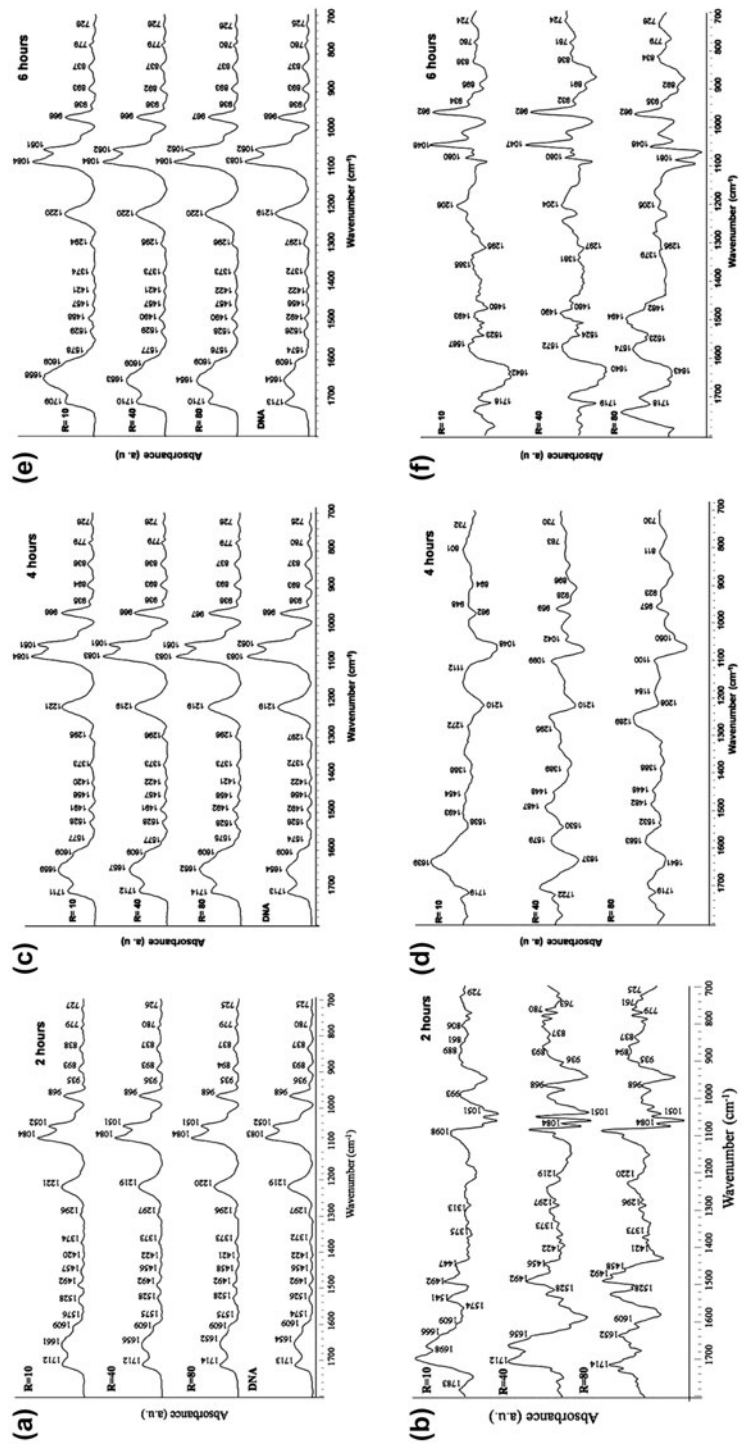

Figure 5. Upper panel exhibits stacked view of FTIR spectra of free calf thymus DNA and its complexes with chloroethyl nitrosourea derivative semustine at different molar ratios as a function of incubation period (a) at 2 h, (c) at 4 h, and (e) at 6 h. Lower panel illustrates corresponding difference spectra of semustine–DNA complexes (b) at 2 h, (d) at 4 h, and (f) at 6 h. All the spectral were collected in the region of 1800 to 700 cm^{-1} .

$$\Delta G_{obs} = -(1.987) \times (298.15) \times \ln(1.53 \times 10^3)$$
$$= -4.35 \text{ kcal/mol}$$

While for lomustine K_a is 8.12×10^3 M^{-1} and hence:

$$\Delta G_{obs} = -(1.987) \times (298.15) \times \ln (8.12 \times 10^3)$$
$$= -5.33 \text{ kcal/mol}$$

These calculated binding energies are consistent to that of predicted by molecular docking simulations (Table 2) of lomustine (–6.36 kcal/mol) and semustine (–4.4 kcal/mol) (Morris et al., 1998).

Comparison of semustine–DNA and lomustine–DNA adducts

Semustine and lomustine both interact with DNA via its nitrogenous bases. Effect of lomustine is found to be more pronounced than semustine as apparent from its overall larger effect on guanine and cytosine bases in terms of infrared spectral shifts and intensity variation (Agarwal et al., 2014). The binding free energy values of the docked semustine–DNA and lomustine–DNA complexes (Table 2) provide another evidence for the stronger DNA-binding affinity of lomustine (–6.36 kcal/mol)

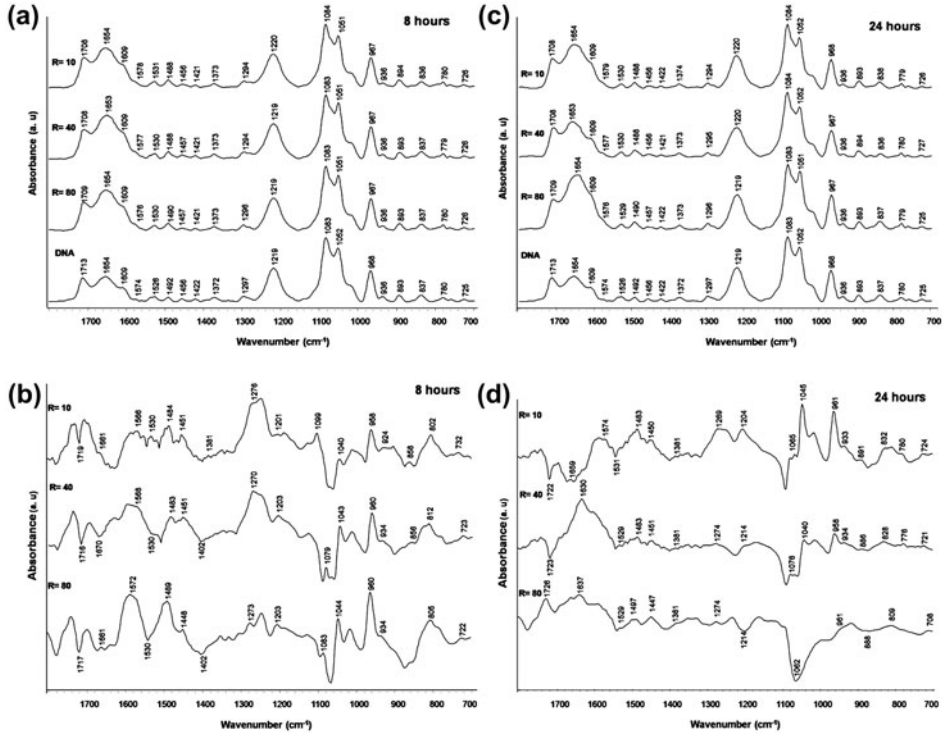

Figure 6. FTIR spectra of free calf thymus DNA and its complexes with chloroethyl nitrosourea derivative semustine in region of 1800 to 700 cm^{-1} at different molar ratios after (a) 8 h and (c) 24 h of incubation periods (upper section). Lower section demonstrates parallel difference spectra of semustine–DNA complexes (b) at 8 h and (d) at 24 h.

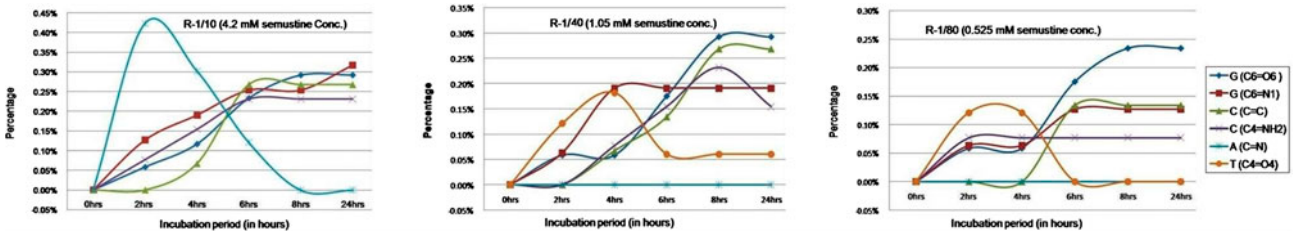

Figure 7. Percentage effect of semustine binding on DNA nitrogenous bases guanine (C6=O6 at 1713 cm^{-1} and C6=N1 bonds at 1574 cm^{-1}), cytosine (C=C at 1492 cm^{-1} and C4=NH2 bonds at 1297 cm^{-1}), adenine (C=N at 1609 cm^{-1}) and, thymine (C4=O4 at 1654 cm^{-1}), estimated as a function of semustine concentration and incubation time.

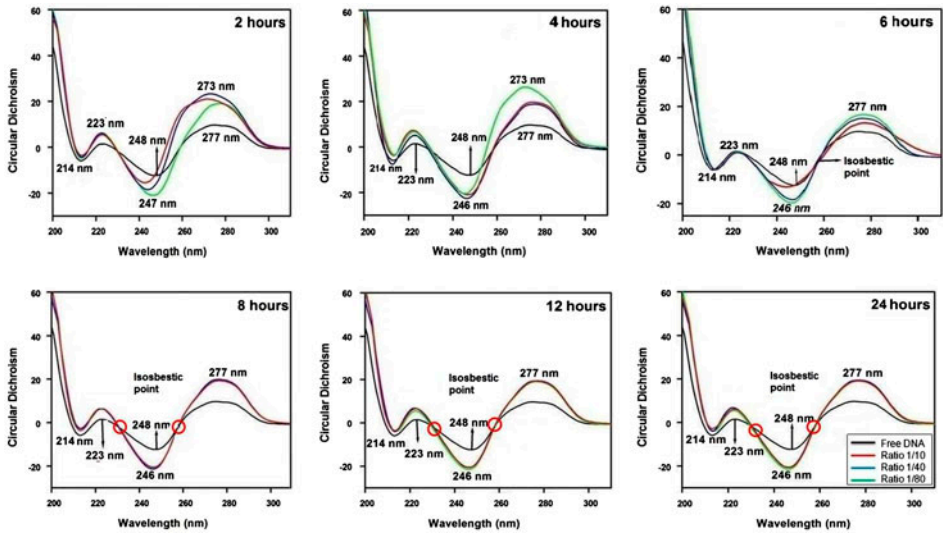

Figure 8. Circular dichroism spectra of free DNA and semustine–DNA complexes at different molar ratios 1/10 (red line), 1/40 (blue line), and 1/80 (green line) against various incubation periods. Here, red circles exemplify the existence of isosbestic point.

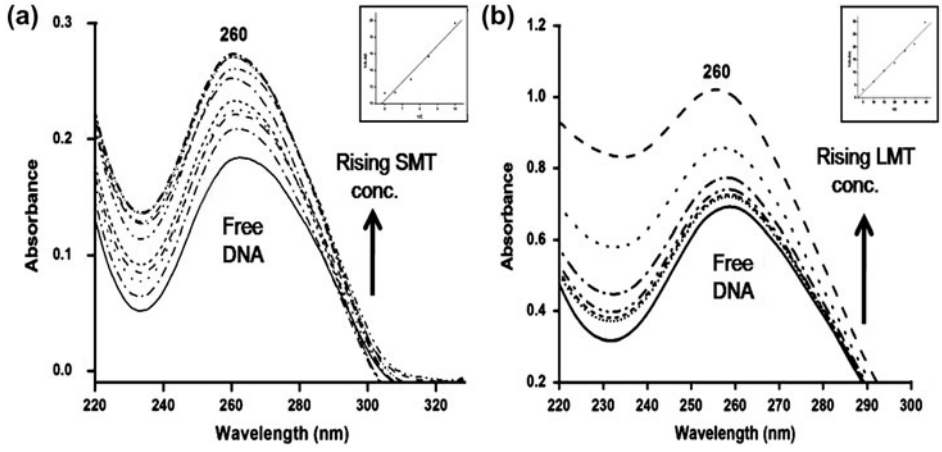

Figure 9. UV–visible spectra of free calf thymus DNA (.2 mM) in the absence and presence of semustine (a) and lomustine (b). Intersect shows double-reciprocal plot of drug binding to DNA. A_0 and A is the absorption of DNA at 260 nm in free and complexed state, respectively. C is the analytical concentration of drug in solution.

than that of semustine (–4.4 kcal/mol), as more negative value of binding energy is an indication of more potent binding of the ligand with its receptor (Zheng et al., 2014). Besides this, infrared results suggest the interaction of lomustine with guanine and cytosine bases of DNA, which draw a parallel understanding with the molecular docking outcomes (Figure 2(d)) (Agarwal et al., 2014). However, semustine initially binds to thymine residues as indicated by docked conformation (Figure 2(b)) and spectral shift in combination with intensity variation at 1654 cm^{-1} infrared band (Figure 5). Both CENUs interact with DNA sugar–phosphate backbone to some extent, which augments their binding and may facilitates proper positioning of CENUs on DNA for their subsequent cytotoxic action. Moreover, in the lomustine–DNA molecular docking simulation of 100 runs, lomustine exhibited 65 conformers in DNA minor groove and 35 conformers in major groove of DNA (under same docking conditions as used for semustine). This illustrates that lomustine plausibly binds in DNA minor groove, whereas semustine preferentially binds in DNA major groove (Figure 3). The lomustine–DNA docked model exhibited two hydrogen bonds formed between the lomustine and guanine (Figure 2(d)). The hydrogen atom at 12th position of lomustine forms hydrogen bond (donor) with O4′ of deoxyribose sugar

moiety linked to guanine at 22nd position (acceptor) with distance of 2.09 Å, whereas oxygen atom at 2nd position of ligand (acceptor) is interacting with guanine (H3) at 22nd position (donor) with 2.037 Å distance. CD spectral profile depicts the difference in the binding pattern of two CENUs with respect to conformational transition in DNA. Lomustine interaction with DNA induces alterations in native B-conformation of DNA related to local base-pair geometry and stimulates transition from B- to A-form (Agarwal et al., 2014). However, upon semustine–DNA complexation, DNA hydration value is lowered and induces some C-form features followed by the formation of a transitional B–C-conformation. Although not much difference is observed in the binding constants of both the CENUs–DNA complexes, overall effect on the structure of DNA is found to be more for lomustine between the two CENUs studied. These outcomes may be helpful in addressing the issues of *structure-based activity* of both CENUs and investigations related to more potency of lomustine than semustine in spite of little difference in their chemical structure.

Conclusion

In the present work, we carried out molecular docking and spectroscopic investigations on the binding properties of chloroethyl nitrosourea derivative semustine with DNA duplex. FTIR spectral outcomes suggest primarily binding of semustine with thymine followed by dG-dC DNA cross-link formation, which further authenticate molecular modeling prediction. Moreover, minor external binding of semustine with phosphate–sugar backbone of DNA is also indicated by FTIR spectral results. Binding energy for semustine–DNA interaction is predicted to be –4.4 kcal/mol, revealing dominance of van der Waals, hydrogen bond, and hydrophobic forces over electrostatic interactions for semustine–DNA complexation. CD spectroscopic data indicate the formation of an intermediary form of DNA during the transition from B- to C-form locally after semustine–DNA complexation, although overall DNA remains in native B-form. Furthermore, DNA-binding mechanism of semustine is compared with that of lomustine. This suggests that lomustine has more prominent effect than semustine with respect to their interaction with DNA double helix. These findings may add further understanding about the action mechanism of chloroethyl nitrosourea derivative at molecular level.

Abbreviations

UV	Ultraviolet
CENUs	chloroethyl nitrosoureas
CD	circular dichroism
CCNU	[1-(2-chloroethyl)-3-cyclohexyl-1-nitrosourea]
ICLs	interstrand cross-links
RMSD	root-mean-square deviation
PDB	Protein Data Bank

Acknowledgment

The authors thank Director, CSIR-National Physical Laboratory, New Delhi, India, for granting the permission for publication of the work. S. A. is thankful to Council of Scientific & Industrial Research, New Delhi, India, for financial support.

References

Agarwal, S., Jangir, D. K., & Mehrotra, R. (2013). Spectroscopic studies of the effects of anticancer drug mitoxantrone interaction with calf-thymus DNA. *Journal of Photochemistry and Photobiology B: Biology, 120*, 177–182.

Agarwal, S., Jangir, D. K., Mehrotra, R., Lohani, N., & Rajeswari, M. (2014). A structural insight into major groove directed binding of nitrosourea derivative nimustine with DNA: A spectroscopic study. *PLoS ONE, 9*, e104115.

Agarwal, S., Jangir, D. K., Singh, P., & Mehrotra, R. (2014). Spectroscopic analysis of the interaction of lomustine with calf thymus DNA. *Journal of Photochemistry and Photobiology B: Biology, 130*, 281–286.

Ahmad, R., Arakawa, H., & Tajmir-Riahi, H. (2003). A comparative study of DNA complexation with Mg(II) and Ca (II) in aqueous solution: Major and minor grooves bindings. *Biophysical Journal, 84*, 2460–2466.

Aksel, T., Majumdar, A., & Barrick, D. (2011). The contribution of entropy, enthalpy, and hydrophobic desolvation to cooperativity in repeat-protein folding. *Structure, 19*, 349–360.

Alex, S., & Dupuis, P. (1989). FT-IR and Raman investigation of cadmium binding by DNA. *Inorganica Chimica Acta, 157*, 271–281.

Bai, B.-Q., Zhao, L.-J., & Zhong, R.-G. (2010). Analysis of deoxyribonucleic acid interstrand cross-links induced by nitrosourea with high performance liquid chromatography-electrospray ionization tandem mass spectrometry. *Chinese Journal of Analytical Chemistry, 4*, 532–536.

Bai, B., Zhao, L., & Zhong, R. (2011). Quantification of meC-CNU-induced dG-dC crosslinks in oligonucleotide duplexes by liquid chromatography/electrospray ionization tandem mass spectrometry. *Rapid Communications in Mass Spectrometry, 25*, 2027–2034.

Banerjee, S., Bright, S. A., Smith, J. A., Burgeat, J., Martínez-Calvo, M., Williams, D. C., Kelly, J. M., & Gunnlaugsson, T. (2014). A supramolecular approach to enantioselective DNA recognition using enantiomerically resolved cationic 4-Amino-1, 8-naphthalimide based Tröger's bases. *The Journal of Organic Chemistry, 79*, 9272–9283.

Banyay, M., Sarkar, M., & Gräslund, A. (2003). A library of IR bands of nucleic acids in solution. *Biophysical Chemistry, 104*, 477–488.

Berman, H. M. & Schneider, B. (1999). *Nucleic acid hydration. Handbook of nucleic acid structure*. S. Neidle, ed. London: Oxford University.

Boice, J. D., Jr, Greene, M. H., Killen, J. Y., Jr, Ellenberg, S. S., Keehn, R. J., McFadden, E., … Fraumeni, J. F., Jr (1983). Leukemia and preleukemia after adjuvant treatment of gastrointestinal cancer with semustine (Methyl-CCNU). *New England Journal of Medicine, 309*, 1079–1084.

Bokma, J. T., Curtis, W. J., & Blok, J. (1987). CD of the li-salt of DNA in ethanol/water mixtures: Evidence for the B-to C-form transition in solution. *Biopolymers, 26*, 893–909.

Brahms, S., Brahms, J., & Van Holde, K. (1976). Nature of conformational changes in poly[d(A-T)-d(A-T)] in the premelting region. *Proceedings of the National Academy of Sciences, 73*, 3453–3457.

Brahms, J., Pilet, J., Lan, T.-T. P., & Hill, L. (1973). Direct evidence of the C-like form of sodium deoxyribonucleate. *Proceedings of the National Academy of Sciences, 70*, 3352–3355.

Braun, C. S., Jas, G. S., Choosakoonkriang, S., Koe, G. S., Smith, J. G., & Middaugh, C. R. (2003). The structure of DNA within cationic lipid/DNA complexes. *Biophysical Journal, 84*, 1114–1123.

Chaires, J. B. (1998). Drug – DNA interactions. *Current Opinion in Structural Biology, 8*, 314–320.

Chan, A., Kilkuskie, R., & Hanlon, S. (1979). Correlations between the duplex winding angle and the circular dichroism spectrum of calf thymus DNA. *Biochemistry, 18*, 84–91.

Connors, K. (1991). *Binding constants: The measurement of molecular complex stability 1987* (Chap 4, pp. 141–188). Ann Arbor, MI: University of Michigan.

Degtyareva, N. N., Wallace, B. D., Bryant, A. R., Loo, K. M., & Petty, J. T. (2007). Hydration changes accompanying the binding of Minor groove ligands with DNA. *Biophysical Journal, 92*, 959–965.

Glasel, J. (1995). Validity of nucleic acid purities monitored by 260 nm/280 nm absorbance ratios. *BioTechniques, 18*, 62–63.

Gombar, C. T., Tong, W. P., & Ludlum, D. B. (1980). Mechanism of action of the nitrosoureas—IV. *Biochemical Pharmacology, 29*, 2639–2643.

González-Ruiz, V., Olives, A. I., Martín, M. A., Ribelles, P., Ramos, M. T., & Menéndez, J. C. (2011). An overview of analytical techniques employed to evidence drug-DNA interactions. Applications to the design of genosensors. *Biomedical Engineering, Trends, Research and Technologies* (Chap. 3, pp. 65–90). Rijeka: InTech.

Goodsell, D. S., Morris, G. M., & Olson, A. J. (1996). Automated docking of flexible ligands: Applications of autodock. *Journal of Molecular Recognition, 9*, 1–5.

Haq, I., & Ladbury, J. (2000). Drug–DNA recognition: energetics and implications for design. *Journal of Molecular Recognition, 13*, 188–197.

Hayes, M. T., Bartley, J., Parsons, P. G., Eaglesham, G. K., & Prakash, A. S. (1997). Mechanism of Action of Fotemustine, a New Chloroethylnitrosourea Anticancer Agent: Evidence for the Formation of Two DNA-Reactive Intermediates Contributing to Cytotoxicity. *Biochemistry, 36*, 10646–10654.

Huang, C. C., Couch, G. S., Pettersen, E. F., & Ferrin, T. E. (1996). Chimera: An extensible molecular modeling application constructed using standard components. *Pacific Symposium on Biocomputing, San Francisco, 1*, 1519–1523.

Huang, S.-Y., & Zou, X. (2010). Inclusion of solvation and entropy in the knowledge-based scoring function for protein−ligand interactions. *Journal of Chemical Information and Modeling, 50*, 262–273.

Huey, R., & Morris, G. M. (2008). *Using AutoDock 4 with AutoDockTools: A Tutorial* (pp. 54–56). La Jolla, CA: The Scripps Research Institute.

Irwin, J. J., Sterling, T., Mysinger, M. M., Bolstad, E. S., & Coleman, R. G. (2012). ZINC: A free tool to discover chemistry for biology. *Journal of Chemical Information and Modeling, 52*, 1757–1768.

Jangir, D. K., Charak, S., Mehrotra, R., & Kundu, S. (2011). FTIR and circular dichroism spectroscopic study of interaction of 5-fluorouracil with DNA. *Journal of Photochemistry and Photobiology B: Biology, 105*, 143–148.

Jangir, D. K., Kundu, S., & Mehrotra, R. (2013). Role of minor groove width and hydration pattern on amsacrine interaction with DNA. *PLoS ONE, 8*, e69933.

Johnson, W. (1994). CD of nucleic acids. *Circular Dichroism: Principles and Applications* (pp. 523–540). New York: Wiley & Sons.

Kankia, B. I., Barany, G., & Musier-Forsyth, K. (2005). Unfolding of DNA quadruplexes induced by HIV-1 nucleocapsid protein. *Nucleic Acids Research, 33*, 4395–4403.

Kennard, O. (1993). DNA-drug interactions. *Pure and Applied Chemistry, 65*, 1213–1222.

Kypr, J., Kejnovská, I., Renčiuk, D., & Vorlíčková, M. (2009). Circular dichroism and conformational polymorphism of DNA. *Nucleic Acids Research, 37*, 1713–1725.

Lenglet, G., & David-Cordonnier, M.-H. (2010). DNA-destabilizing agents as an alternative approach for targeting DNA: Mechanisms of action and cellular consequences. *Journal of Nucleic Acids, 2010*, 1–17.

Li, Z. (2012). *The kinetics and mechanisms of some fundamental organic reactions of nitro compounds*. All Graduate Theses and Dissertations: Paper 1407. Utah State University Libraries, Logan, UT.

Loprete, D., & Hartman, K. (1993). Conditions for the stability of the B, C, and Z structural forms of poly(dG-dC) in the presence of lithium, potassium, magnesium, calcium, and zinc cations. *Biochemistry, 32*, 4077–4082.

Mayer, R. G., & Drago, R. S. (1976). Interpretation of isosbestic points. *Inorganic Chemistry, 15*, 2010–2011.

McCann, J. J., Lo, T. M., & Webster, D. (1971). Cross-linking of DNA by alkylating agents and effects on DNA function in the chick embryo. *Cancer Research, 31*, 1573–1579.

McCormick, J. E., & Stanley McElhinney, R. (1990). Nitrosoureas from chemist to physician: Classification and recent approaches to drug design. *European Journal of Cancer and Clinical Oncology, 26*, 207–221.

Mehrotra, R., Jangir, D., Agarwal, S., Ray, B., Singh, P., & Srivastava, A. K. (2013). Interaction studies of anticancer drug lomustine with calf thymus DNA using surface enhanced Raman spectroscopy. *MAPAN, 28*, 273–277.

Miyagami, M., Tsubokawa, T., Tazoe, M., & Kagawa, Y. (1990). Intra-arterial ACNU chemotherapy employing 20% mannitol osmotic blood-brain barrier disruption for malignant brain tumors. *Neurologia Medico-Chirurgica, 30*, 582–590.

Miyahara, T., Nakatsuji, H., & Sugiyama, H. (2012). Helical structure and circular dichroism spectra of DNA: A theoretical study. *The Journal of Physical Chemistry A, 117*, 42–55.

Morris, G., Goodsell, D., Halliday, R., Huey, R., Hart, W., Belew, R., & Olson, A. (1998). Automated docking using a Lamarckian genetic algorithm and an empirical binding free energy function. *Journal of Computational Chemistry, 19*, 1639–1662.

Morris, G. M., Goodsell, D. S., Halliday, R. S., Huey, R., Hart, W. E., Belew, R. K., & Olson, A. J. (1998). Automated docking using a Lamarckian genetic algorithm and an empirical binding free energy function. *Journal of Computational Chemistry, 19*, 1639–1662.

Morris, G. M., Huey, R., Lindstrom, W., Sanner, M. F., Belew, R. K., Goodsell, D. S., & Olson, A. J. (2009). AutoDock4 and AutoDockTools4: Automated docking with selective receptor flexibility. *Journal of Computational Chemistry, 30*, 2785–2791.

Naghipur, A., Ikonomou, M. G., Kebarle, P., & Lown, J. W. (1990). Mechanism of action of (2-haloethyl)nitrosoureas on DNA: discrimination between alternative pathways of DNA base modification by 1,3-bis(2-fluoroethyl)-1-nitrosourea by using specific deuterium labeling and identification of reaction products by HPLC/tandem mass spectrometry. *Journal of the American Chemical Society, 112*, 3178–3187.

Nandy, A., & Basak, S. C. (2010). New approaches to drug–DNA interactions based on graphical representation and numerical characterization of DNA sequences. *Current Computer-Aided Drug Design, 6*, 283–289.

Neidle, S., Rayner, E. L., Simpson, I. J., Smith, N. J., Mann, J., Baron, A., … Kelland, L. R. (1999). Symmetric bisbenzimidazoles: new sequence-selective DNA-binding molecules. *Chemical Communications, 10*, 929–930.

O'Boyle, N. M., Banck, M., James, C. A., Morley, C., Vandermeersch, T., & Hutchison, G. R. (2011). Open Babel: An open chemical toolbox. *Journal of cheminformatics, 3*, 1–14.

Patil, S. D., & Rhodes, D. G. (2000). Conformation of oligodeoxynucleotides associated with anionic liposomes. *Nucleic Acids Research, 28*, 4125–4129.

Pohle, W., Selle, C., Gauger, D. R., Zantl, R., Artzner, F., & Rädler, J. O. (2000). FTIR spectroscopic characterization of a cationic lipid–DNA complex and its components. *Physical Chemistry Chemical Physics, 2*, 4642–4650.

Portugal, J., & Subirana, J. (1985). Counterions which favour the C form of DNA. *The EMBO journal, 4*, 2403–2408.

Puyo, S., Montaudon, D., & Pourquier, P. (2013). From old alkylating agents to new minor groove binders. *Critical Reviews in Oncology/Hematology, 89*, 43–61.

Rueda, L., Banerjee, S., Aziz, M. M., & Raza, M. (2010). Protein–protein interaction prediction using desolvation energies and interface properties. *IEEE International Conference on Bioinformatics and Biomedicine (BIBM), 17*, 18–21.

Sanner, M. F. (1999). Python: A programming language for software integration and development. *Journal of Molecular Graphics and Modelling, 17*, 57–61.

Schabel, F., Jr (1976). Nitrosoureas: A review of experimental antitumor activity. *Cancer Treatment Reports, 60*, 665–698.

Schallreuter, K. U., Gleason, F. K., & Wood, J. M. (1990). The mechanism of action of the nitrosourea anti-tumor drugs on thioredoxin reductase, glutathione reductase and ribonucleotide reductase. *Biochimica et Biophysica Acta (BBA)-Molecular Cell Research, 1054*, 14–20.

Snyder, R. D., Holt, P. A., Maguire, J. M., & Trent, J. O. (2013). Prediction of noncovalent Drug/DNA interaction using computational docking models: Studies with over 1350 launched drugs. *Environmental and Molecular Mutagenesis, 54*, 668–681.

Strange, P. G. (1996). The energetics of ligand binding at catecholamine receptors. *Trends in Pharmacological Sciences, 17*, 238–244.

Tang, W., Zhao, L.-J., & Zhong, R.-G. (2008). Agarose gel electrophoresis and fluorometric assays for the determination of DNA cross-linking induced by semustine. *The 2nd IEEE International Conference on Bioinformatics and Biomedical Engineering (ICBBE)*, 322, 16–18.

Tong, W. P., Kirk, M. C., & Ludlum, D. B. (1983). Mechanism of action of the nitrosoureas – V: Formation of O6-(2-fluoroethyl) guanine and its probable role in the crosslinking of deoxyribonucleic acid. *Biochemical Pharmacology, 32*, 2011–2015.

Tyagi, G., Charak, S., & Mehrotra, R. (2012). Binding of an indole alkaloid, vinblastine to double stranded DNA: A spectroscopic insight in to nature and strength of interaction. *Journal of Photochemistry and Photobiology B: Biology, 108*, 48–52.

Tyagi, G., Jangir, D. K., Singh, P., & Mehrotra, R. (2010). DNA Interaction Studies of an anticancer plant alkaloid, vincristine, using Fourier transform infrared spectroscopy. *DNA and Cell Biology, 29*, 693–699.

Vijayalakshmi, R., Kanthimathi, M., Subramanian, V., & Nair, B. U. (2000). DNA Cleavage by a Chromium(III) Complex. *Biochemical and Biophysical Research Communications, 271*, 731–734.

Woods, K. K., Lan, T., McLaughlin, L. W., & Williams, L. D. (2003). The role of minor groove functional groups in DNA hydration. *Nucleic Acids Research, 31*, 1536–1540.

Zhang, Z., Huang, W., Tang, J., Wang, E., & Dong, S. (2002). Conformational transition of DNA induced by cationic lipid vesicle in acidic solution: spectroscopy investigation. *Biophysical Chemistry, 97*, 7–16.

Zhao, L., Li, L., Xu, J., & Zhong, R. (2014). Comparative investigation of the DNA inter-strand crosslinks induced by ACNU, BCNU, CCNU and FTMS using high-performance liquid chromatography–electrospray ionization tandem mass spectrometry. *International Journal of Mass Spectrometry, 368*, 30–36.

Zhao, L.-J., Ren, T., Bai, B.-Q., Zhang, R., & Zhong, R.-G. (2011). Comparative investigations of deoxyribonucleic acid interstrand crosslinks induced by semustine using fluorescence and high performance liquid chromatography–mass spectrometry. *Chinese Journal of Analytical Chemistry, 4*, 476–480.

Zhao, L., Zhong, R., & Zhen, Y. (2007). An ONIOM study on the crosslinked base pairs in DNA reacted with chloroethylnitrosoureas. *Journal of Theoretical & Computational Chemistry, 6*, 631–639.

Zheng, K., Liu, F., Xu, X.-M., Li, Y.-T., Wu, Z.-Y., & Yan, C.-W. (2014). Synthesis, structure and molecular docking studies of dicopper (ii) complexes bridged by N-phenolato-N′-[2-(dimethylamino) ethyl] oxamide: The influence of terminal ligands on cytotoxicity and reactivity towards DNA and protein BSA. *New Journal of Chemistry, 38*, 2964–2978.